Suitability of SIMP and BESO Topology Optimization Algorithms for Additive Manufacture

Aremu A., Ashcroft I., Hague R., Wildman R., Tuck C.
Wolfson School of Mechanical and Manufacturing Engineering,
Loughborough University, Loughborough, LE11 3TU, UK

Reviewed, accepted September 23, 2010

Abstract

Additive manufacturing (AM) is expanding the range of designable geometries, but to exploit this evolving design space new methods are required to find optimum solutions. Finite element based topology optimisation (TO) is a powerful method of structural optimization, however the results obtained tend to be dependent on the algorithm used, the algorithm parameters and the finite element mesh. This paper will discuss these issues as it relates to the SIMP and BESO algorithms. An example of the application of topological optimization to the design of improved structures is given.

Nomenclature

FR	=	Filter radius
ER	=	Evolution rate
VF	=	Volume Fraction
η_b	=	Sensitivity of node *b*
V_a	=	Volume of element *a*
λ_a	=	Sensitivity of element *a*
s	=	Number of elements connected to node
V_{m+1}	=	Iterative new target volume
V_m	=	Current volume
d_{ab}	=	Distance between centre of an element *a* and node *b*
λ_{del}^{th}	=	Element sensitivity threshold value (deleting)
λ_{add}^{th}	=	Element sensitivity threshold value (adding)
tol	=	Convergence tolerance, 1e-5
m	=	Current iteration number
T	=	Number of iterations over which convergence is measured, 5
E_s	=	Young's Modulus Solid
E_v	=	Young's Modulus Void
TO	=	Topology Optimization
V*	=	Volume fraction constraint
SE	=	Strain Energy
ΔSE	=	change in strain energy
y	=	Distance between the centre and a node of same element.
u_e	=	Elemental displacement vector
k_e	=	Elemental stiffness matrix
P	=	Penalization factor
x_e	=	Elemental density distribution

μ_m = Displacement field at iteration m

$\rho_{\min}$ = Parameter used to prevent singularity

ρ_m = Density at the previous cycle

ζ = Move limit

η = Tuning parameter

Λ_m = Lagrange multiplier at cycle m

$\widehat{H}_f$ = Convolution operator

$L(x, y)$ = Distance between centres of element x and y.

I Introduction

Additive manufacturing (AM) is a relatively recent approach to manufacturing whereby a component is built up [1-3] layer by layer, usually from sliced 3D CAD data. It is a contrasting approach to traditional manufacturing techniques such as subtractive (e.g. machining) or formative (e.g. casting). This layer by layer approach requires less manufacturing constraints. Its ability to build components with intricate complexities opens up the design domain significantly, enabling the production of optimal parts with improved structural performance. Established topology optimization algorithms (TO) could be adopted for AM by relaxing constraints within these algorithms originally meant for traditional manufacturing routes.

TO is a type of structural optimization that seeks the optimum layout of a design by determining the number of members required and the manner in which these members are connected. Unlike shape and size optimization, TO achieve designs that are not greatly constrained by the nature of the initial design. Hence, TO is a better route to take towards optimum parts. Several algorithms have been developed for TO. These include homogenization [4, 5], solid isotropic microstructure with penalization (SIMP) [6-8], and bi-directional evolutionary structural optimization (BESO) [9-11]. Stochastic algorithms used in the broader field of optimization have also been adopted for TO, among which are genetic algorithms [12-14] and ant colony optimization [15]. Optimum topologies depend on which of these algorithm is used, starting design, finite element mesh, parametric settings. A detailed study of these is necessary if AM's design flexibility is to be completely exploited. In this paper, we investigate the effects of these factors on optimum achieved by the SIMP and BESO algorithm, since they have been widely implemented in literature to achieve practical designs.

II Method

SIMP and BESO are the most widely used TO algorithms, owing to their efficiency and simplicity. The section describes the main features of these two algorithms.

A BESO

The BESO algorithm is a combination of additive evolutionary structural optimization (AESO) [9] and evolutionary structural optimization (ESO) [16]. Querin et al [9, 11] originally proposed and implemented BESO to improve results and

convergence time of both AESO and ESO. Huang and Xie [10] presented a different version to BESO to solve compliance problems. BESO is a finite element based TO method, where inefficient material is iteratively removed from a structure as efficient material is simultaneously added to the structure. Figure 1 show a BESO flow chart for the minimization of strain energy (*SE*) for a given volume fraction constraint (V*). An evolution rate (ER), filter radius (FR), V* and design domain are supplied to the algorithm. The ER is the rate at which the volume is allowed to change per iteration. FR is a distance limit. Sensitivity values of nodes within FR from the centre of an element are used to recalculate elemental sensitivity values of the same element when filtering sensitivities. This is done to eliminate the occurrence of undesired checkerboard patterns in optima.

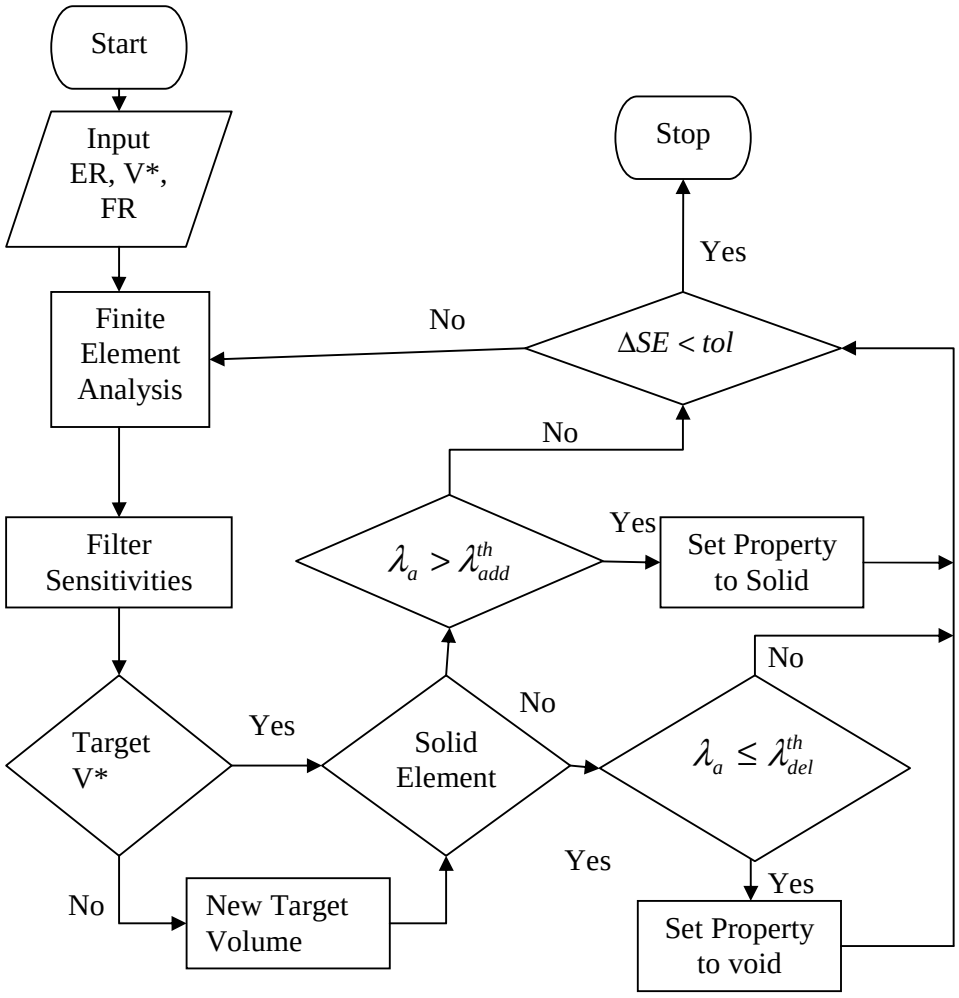

Figure 1: BESO Flow chart

The design domain is discretized and a finite element analysis (FEA) is performed. An initially fully (fig 2a) or partially (fig 2b) solid design domain has often been used in past works. Where a partially solid design domain has been used, the solid elements have been concentrated in a particular region of the design domain. ***This sort of starting design is intuitive in nature and might have constrained the***

topology to a local minimum. This is illustrated later by stochastically distributing solid elements in the design domain.

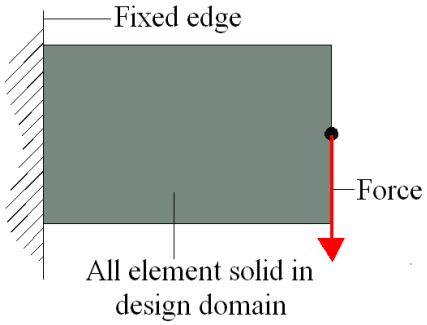

(a)

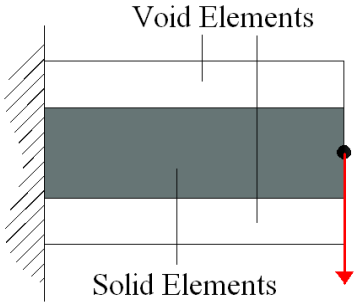

(b)

Fig 2: Starting designs (a) fully solid start design
(b) Partially solid start design

Elemental sensitivities are then filtered by first distributing them into nodes, to which they are connected using equation 1,

$$\eta_b = \frac{\sum_{a=1}^{s} V_a \lambda_a}{\sum_{a=1}^{s} V_a} \qquad (1)$$

The sensitivity of node *b*, η_b is computed by finding all elements *a* connected to this node, and averaging their sensitivities values λ_a according to equation 1. Elemental sensitivities are then recomputed by finding nodes whose distance to the centre of an element *a*, is less than or equal to FR. Sensitivity values of these nodes are averaged according to equation 2 to obtain elemental sensitivity values.

$$\lambda_a = \frac{\sum_{b=1}^{s} v(d_{ab}) \eta_b^c}{\sum_{b=1}^{s} v(d_{ab})} \qquad (2)$$

Where $v(d_{ab}) = FR - d_{ab}$. ***Structural detail might be lost while eliminating checkerboards in this manner***. These filtered sensitivities are averaged with values they assumed in the previous optimization iteration to further improve these sensitivities. The volume fraction (VF) of the design domain is checked against the target volume fraction *V**, if they were not equal a new iterative target volume is computed equation 3,

$$V_{m+1} = V_m(1 \pm \mathrm{ER}) \tag{3}$$

Elemental sensitivity values can then be ranked. Solid elements having sensitivity values below λ_{del}^{th} are reclassified as having void property. Void elements have been modelled in this work by multiplying the elemental stiffness matrix of element concerned by 1e-12. This is done to reduce the stiffness contribution of these elements before the global stiffness matrix is assembled. Reducing the structural stiffness this way is a soft kill approach to TO. This has been adopted in this work to avoid connectivity problems associated with hard kill [10] optimization procedures. The numbers of void elements reclassified as solid brings the current volume of solid elements to V_{m+1} at iteration m. The TO is repeated until ΔSE is less than a specified tolerance (*tol*) and the specified volume fraction is reached. ΔSE is computed using equation 4,

$$\Delta SE = \frac{\left| \sum_{i=1}^{T} \left(SE_{m-i+1} - SE_{m-T-i+1} \right) \right|}{\sum_{i=1}^{T} SE_{m-1+1}} \tag{4}$$

The mesh does not change from the start to the end of the TO. BESO algorithm might be constrained by the starting design, ER, FR and the finite element mesh. In the next sections we investigate these effects.

B SIMP

Rozvany et al [7] developed the SIMP algorithm to achieve practical designs for generalized shape optimization (optimization involving higher volume fraction). Figure 3 shows flow chart for the SIMP algorithm to minimize SE for a volume fraction constraint. Sigmund [17] implementation of SIMP is described in this paper. The compliance problem can be expressed mathematically as,

$$\min_x : SE = \sum_{e=1}^{N} (x_e)^p u_e^T k_e u_e \,,$$

$$\text{subject to} \qquad \frac{V(x)}{V_o} = V^* \qquad 0 < \rho_{\min} \le x_e \le 1 \tag{5}$$

The penalty factor *P* is a main feature of the SIMP algorithm. This factor suppresses the occurrence of fractional densities in the optimum design. Its inclusion has been justified by assuming a high expense of making fractional densities.

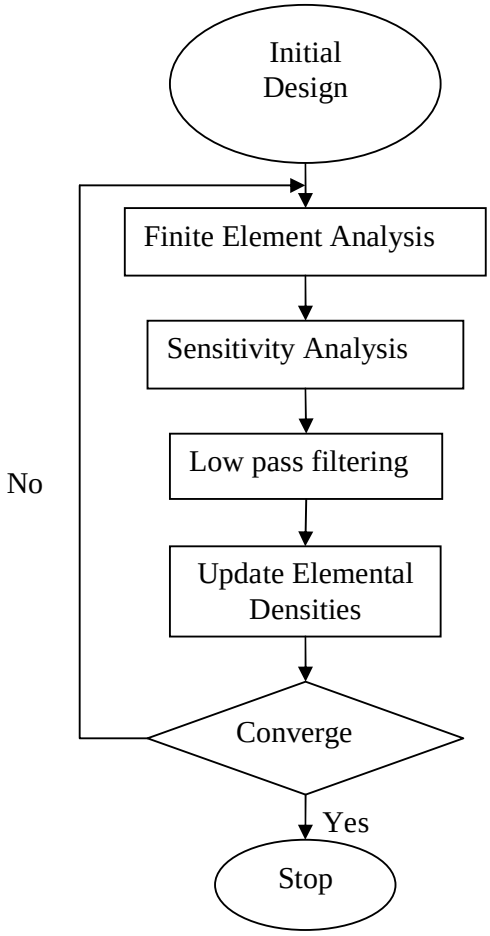

Figure 3: SIMP flow chart

According to Zhou and Rozvany [6], ***"the extra manufacturing cost of cavities would increase with the size of the cavities if we consider a casting process requiring some sort of formwork for the cavities".*** This is not true for AM, since manufacturing cost of AM is independent [2] of part complexity. Most commercial TO software have implemented SIMP for TO, hence raising questions about their suitability for AM.

An initial distribution of density in the design domain is used as the starting design. Sigmund suggests [17] an initial even distribution of these densities, Bendsoe [4] terms it an initial guess. ***There isn't any rigorous mathematical proof for choosing an even density distribution***. ***It is unclear the sort of initial density distribution implemented in commercial TO software.*** In later sections we investigate the effect of random density distribution. Using these densities, an FEA is performed; the displacement vector from the FEA is used to calculate the SE (equation 6) and sensitivities. These sensitivities are calculated by differentiating equation 6 to get

$$\frac{\partial(SE)}{\partial x_e} = -p(x_e)^{p-1} u_e^T k_e u_e \qquad (6)$$

Sensitivities are filtered to eliminate the existence of checker board patterns in the optima using equation 7,

$$\frac{\hat{\partial}(SE)}{\partial x_e} = \frac{1}{x_e \sum_{f=1}^{N} \hat{H}_f} \sum_{f=1}^{N} \hat{H}_f x_f \frac{\partial(SE)}{\partial x_f} \qquad (7)$$

$$\text{where } H_f = FR - L(x, y)$$

Other methods to eliminate checkerboard patterns [4, 18, 19] include perimeter control, filtering the densities, patch smoothing, image processing, higher order elements and monotonic scale length based control. Each of these techniques bring new challenges into the TO. Filtered sensitivities are then used to update densities using the optimality criteria method as expressed in equation 8. The process is continued until convergence is reached.

$$\rho_{m+1} = \{\max\{(1-\zeta)\rho_m, \rho_{\min}\}\} \text{ If } \rho_m B_m = \{\max\{(1-\zeta)\rho_m, \rho_{\min}\}\}$$
$$\rho_{m+1} = \{\max\{(1+\zeta)\rho_m, 1\}\} \text{ If } \rho_{m+1} = \{\min(1+\zeta)\rho_m, 1\} \le \rho_m, \rho_{\min}$$
$$\text{Otherwise } \rho_{m+1} = B_m^{\eta}\rho_m,$$

$$B_m = \Lambda_m^{-1} p\rho(x)^{p-1} E_{ijkl}^0 \varepsilon_{ij}(u_m)\varepsilon_{kl}(\mu_m) \qquad (8)$$

Again as with BESO, most applications of SIMP in the literature has been with a constant mesh. The continuous change in topology during a TO suggest results might by improved by an iterative mesh improvement.

III 2D Example

A cantilever plate problem (figure 4) is solved to show the effect of the different aspects of the BESO and SIMP algorithm on the optimum topologies.

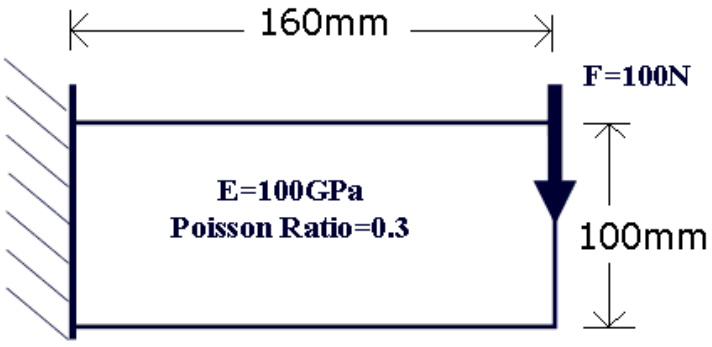

Figure 4: Cantilever plate

The objective is to minimize *SE* for a *VF* constraint of 0.5. The cantilever plate was meshed with 16000 quadrilateral elements. The left side of the plate is fixed while a 100N force is imposed at the middle of the right side of the plate.

A BESO

Figure 5 shows results of BESO algorithm at different parametric settings and starting point. FR was set at 3mm for ER=10% to achieve figure 5a. Reducing both FR and ER to 1mm and 0.5% results in topology shown in figure 5b. Figure 5c is for a random starting point where solid elements are randomly distributed in the design domain. It can be seen from this figure that the parametric settings does affect the nature of an optimal topology since figure 5a and 5c and different.

(a) (b) (c)

Figure 5: BESO topologies
(a) FR=3mm, ER=10%, solid start, SE=1.87Nmm
(b) FR=1mm, ER=0.5%, solid start, SE=1.84Nmm
(c) FR=3mm, ER=1%, random start, SE=1.82Nmm

Also, the random start converged to a different topology with lower SE. Hence the starting point also affects the nature of the optima. Starting with a fully solid domain moved the TO towards a local minimum. Figure 5c might not be the best design possible for this problem as it differ from known Mitchell's [7] analytical solutions to this problem. A detail study of the parameters and starting point might improve the BESO algorithm.

B SIMP

Figure 6 shows the SIMP topologies for different starting points and parametric values. As shown in Figure 6a, a low FR of 1mm does not totally eliminate checkerboard pattern. If both the FR and P are kept at 1 (Figure 6b), checkerboards disappear but there is a large grey region owing to unpenalized intermediate densities. While the main feature of SIMP is to steer TO towards feasible topologies without grey region, there might be an interpretation for intermediate densities in AM as this has the lowest SE. If P=3 and FR=1.5, the grey regions disappear (Figure 6c).

Unlike figure 6(a-c), figure 6d was carried out with a random starting point. As before symmetrical constraint were imposed to attain figure 6d by ensuring the density distribution of the upper half of the plate was a mirror image of the lower half. This topology (figure 6d) is characterized by an SE of 3.8Nmm which is lower than *SE* for figure 6a and 6c where and even density distribution was used at the start of the TO.

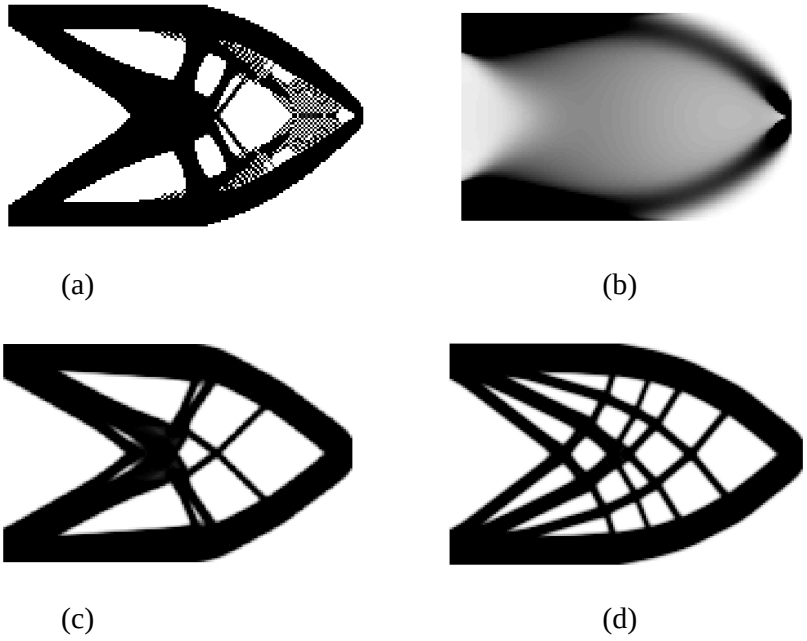

Figure 6: SIMP topologies
(a) P=3, FR=1mm, *SE*=4.0Nmm, 0.5 even density start
(b) P=1, FR=1mm, *SE*=3.3Nmm, 0.5 even density start
(c) P=3, FR=1.5mm, *SE*=3.9Nmm, 0.5 even density start
(d) P=3, FR=1.5mm, *SE*=3.8Nmm, Random density start

IV 3D BESO application

The BESO algorithm is used to solve a practical 3D problem of an aerospace arm shown in figure 7. All degrees of freedom are constrained in surface A, while pressure of 594KPa is imposed on surface B. This arm is meshed with approximately 300,000 tetrahedral elements to investigate the effects of changing FR and ER on the optima. The red part is set to non-design while the green is the design domain.

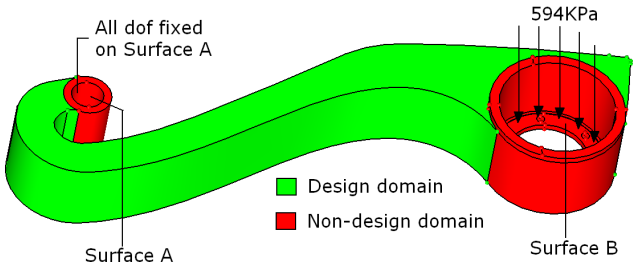

Figure 7: 3D Aerospace metallic arm

Two sets of experiments are conducted, in the first set the ER is set at 5%, while the FR is varied by setting it as a multiple (FRF-filter radius factor) of the distance between the centroid of a tetrahedral element and a node on that element. This factor is set at 1.5, 2.0, 2.5, 3.0. The FRF is fixed at 2.0 while the ER is set at 1%, 3%, 7% and 10% in the second set experiments.

A FR Results

Figure 8 shows the optimum topologies for the different FRF. A plot of *SE* against iteration is shown in figure 9.

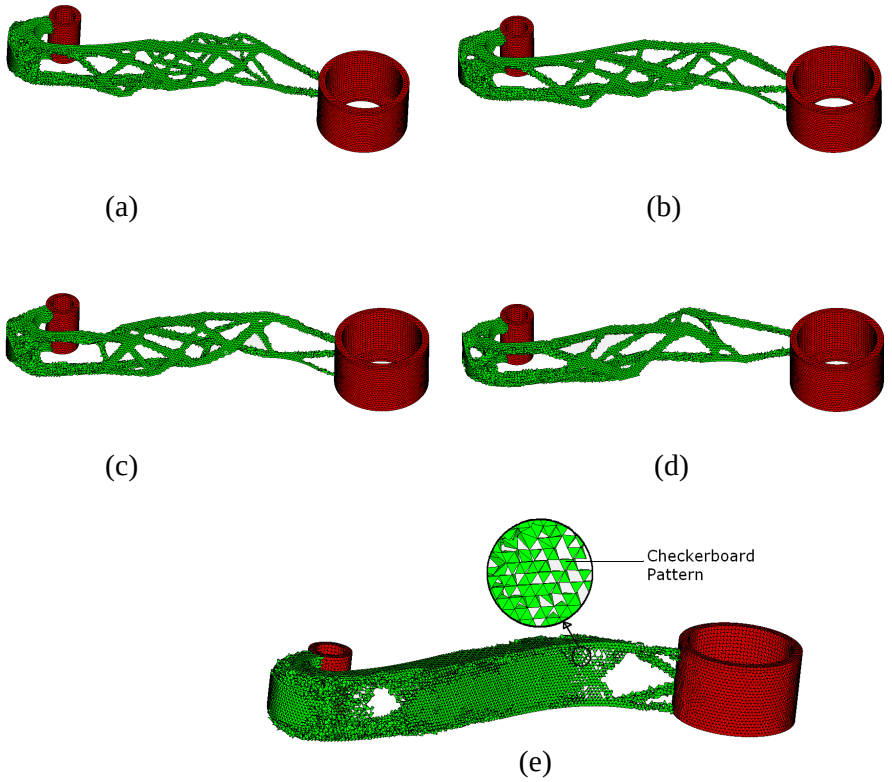

Figure 8: Optimum topologies for FR Experiment (ER=5%)
(a) FRF=1.5, (b) FRF=2.0, (c) FRF=2.5, (d) FRF=3.0 (e) Unfiltered

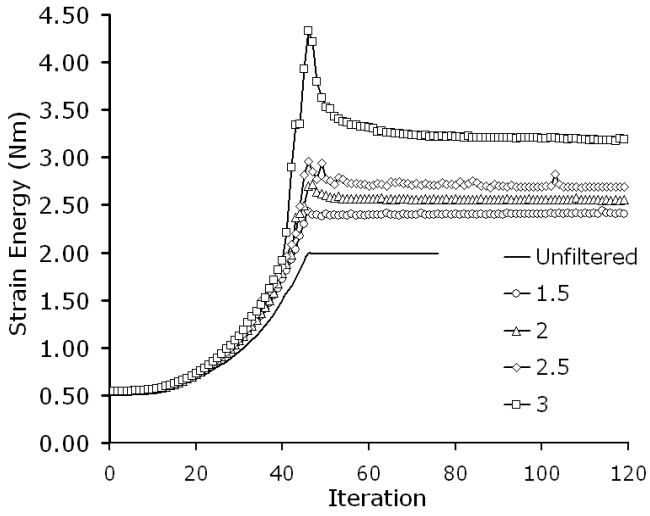

Figure 9: *SE* against iteration (FR)

The Structures appear truss-like but are significant different since the location and number of trusses are significantly different. The number of trusses decrease as the

FRF is increased. This orients the BESO algorithm towards a less optimal part as shown in Figure 9 and 10.

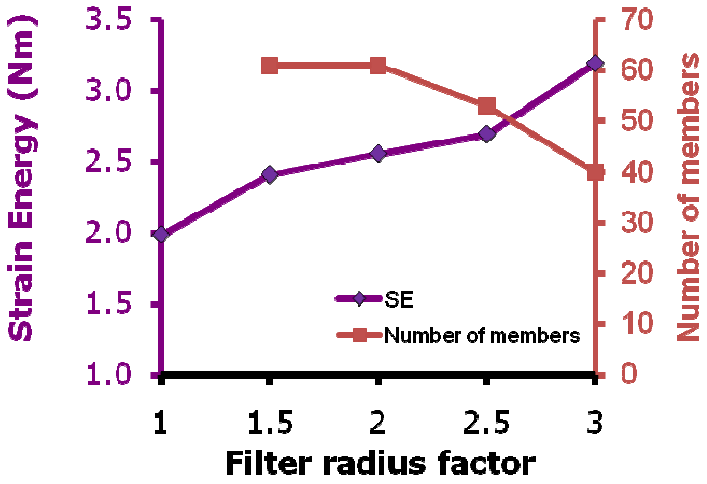

Figure 10: *SE* and Number of members against FRF

B ER Results

Fig 11 shows the results for the ER experiments. Optimum topologies appear truss-like, similar to results for FR experiments. The locations of these trusses are again different, significantly dependent on the ER. Though the graph of *SE* against ER suggest a quadratic relationship (figure 12), the TO is less sensitive to increasing ER as compared to FR.

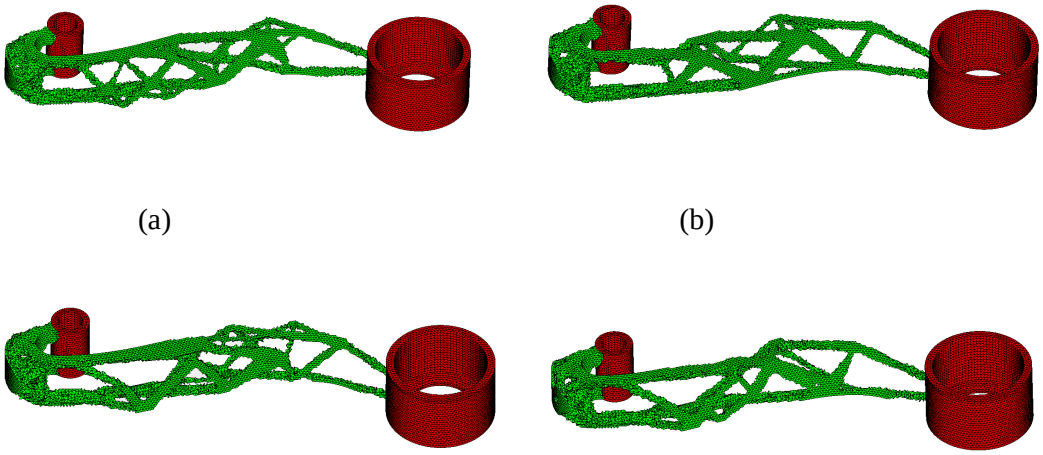

(a) (b)

(b) (d)

Fig 11: Optimum topologies for ER Experiments (FRF=2):
(a) ER=1%, (b) ER=3%, (c) ER=7%, (d) ER=10%

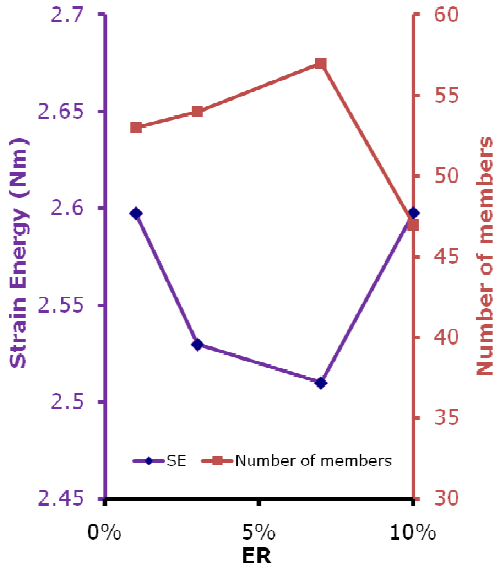

Figure 12: *SE* and Number of members against ER

IV Conclusion

Though BESO and SIMP attains optimal topologies efficiently, these topologies are often local since the TO is constrained by starting design, finite element mesh and parametric values. These less complex optima are suitable for traditional manufacturing; AM's ability to make complex parts allows the production of truly optimal parts. Hence this algorithms needs to be improved for AM.

In the BESO algorithm an increase in FR decrease the complexity in the part and orients the TO towards less optimum topologies. In the three dimensional case, the FR has a greater influence on the TO than the ER. The optimum ER occurs at 6%, though more data point is needed to confirm this.

The basis for inclusion of a penalty factor in the SIMP might be inappropriate for AM, since its manufacturing cost is independent of complexity. A different penalization approach might resolve this problem.

The stagnant mesh often used for the iterative FEA in both BESO and SIMP needs to be improved. Numerical errors might have constrained the TO, since topologies achieved while solving the cantilever problem differ significantly from Michell's analytically optima [7]. Also, the issue of different optima topology for different starting point might have been caused by these errors. While mesh refinement might solve this, computational cost limits resolution attainable. An adaptive mesh improvement strategy could be incorporated in these algorithms to focus refined elements at new boundaries and coarsen mesh away from boundaries. Old void elements could be purge from the design domain to allow the introduction of smaller new elements at the boundaries while reducing computational cost. Further work would investigate these proposed amendments.

These improvement might cause the TO to efficiently attain highly complex topologies with improved performance. These topologies can be made via AM.

References

1. Tuck, C.J., Hague, R.J.M., Ruffo, M., Ransley, M., Adams, P., *Rapid manufacturing facilitated customization.* International Journal of Computer Integrated Manufacturing, 2008. **21**(3): p. 15.

2. Gibson, I., Rosen, D.W., Stucker, B., *Additive Manufacturing Technologies.* 2009, New York: Springer.

3. Hopkinson, N., Hague, R., Dickens, P., *Rapid Manufacturing: An industrial revolution for a digital age*. Book. 2006: John Wiley and Sons. 285.

4. Bendsoe, M.P., Sigmund, O., *Topological optimization: theory, methods and applications.* 2004, Berlin: Springer-Verlag. 370.

5. Bendsoe, M.P., Kikuchi, *Generating optimal topologies in structural design using a homogenization method.* Computer Methods in Applied Mechanics and Engineering, 1988. **71**: p. 28.

6. Zhou, M., Rozvany, G.I.N., *The COC algorithm, Part II: Topological geometrical and generalized shape optimization.* Computer Methods in Applied Mechanics and Engineering, 1991. **89**: p. 28.

7. Rozvany, G.I.N., Zhou, M., Birker, T., *Generalized shape optimization without homogenization.* Structural Optimization, 1992. **4**: p. 3.

8. Rozvany, G.I.N., *A critical review of established methods of structural topology optimization.* Struct Multidisc Optim, 2009. **37**: p. 21.

9. Querin, O.M., Steven, G.P., Xie, Y.M., *Evolutionary Structural optimization using an additive algorithm.* Finite Element in Analysis and Design, 2000a. **34**: p. 18.

10. Huang, X., Xie, Y.M., *Convergent and mesh-independent solutions for the bi-directional evolutionary structural optimization method.* Finite Elements in Analysis and Design, 2007. **43**: p. 11.

11. Querin, O.M., Young V., Steven, G.P., Xie, Y.M., *Computational Efficiency and validation of bi-directional evolutionary structural optimization.* Comput Methods Applied Mechanical Engineering, 2000b. **189**: p. 15.

12. Chapman, C.D., Saitou, K., Jakiela, M.J., *Genetic algorithms as an approach to configuration and topology design.* Journal of Mechanical Design, 1994. **116**(105): p. 8.

13. Chapman, C.D., Jakiela, M.J., *Genetic algorithm-based structural topology design with compliance and topology simplification consideration.* Journal of Mechanical Design, 1996. **118**(89): p. 10.

14. Jakiela, M.J., Chapman, C., Duda, J., Adewuya, A., Saitou, K., *Continuum structural topology design with genetic algorithms.* Computer Methods Applied Mechanics and Engineering, 2000. **186**: p. 18.

15. Luh, G., Lin, C., *Structural topology optimization using Ant colony algorithm.* Applied Soft Computing, 2009. **9**: p. 11.

16. Xie, Y.M., Steven, G.P., *Evolutionary Structural Optimization.* 1997, London: Springer-Verlag.

17. Sigmund, O., *A 99 line topology optimization code written in Matlab.* Struct Multidisc Optim, 2001. **21**: p. 8.

18. Kim. H., Q.O.M., Steven, G.P., *On the development of structural optimization and its relevance in engineering design.* Design studies, 2001. **23**: p. 18.

19. Zhou, M., Shyy Y.K., Thomas, H.L., *Checkboard and minimum member size control in topology optimization.* Struct Multidisc Optim, 2001. **21**: p. 7.